Bull. Mater. Sci. _####################_
https://doi.org/10.1007/s12034-021-02563-7

Synthesis of standing ZnO nanosheets and impact of Ag nanoparticles loading on its optical property

MARJONI IMAMORA ALI UMAR[1,*], SETIA BUDI[2], MUHAMMAD NURDIN[3] and AKRAJAS ALI UMAR[4]

[1]Faculty of Tarbiyah, Department of Physical Education, Insitut Agama Islam Negeri Batusangkar, Batu Sangkar 27213, Indonesia

[2]Faculty of Mathematics and Natural Science, Department of Chemistry, Universitas Negeri Jakarta, DKI, Jakarta 13220, Indonesia

[3]Faculty of Mathematics and Natural Science, Department of Chemistry, Universitas Halu Oleo, Kendari 93232, Indonesia

[4]Institute of Microengeineering and Nanoelectronics, Universiti Kebangsaan Malaysia, UKM, 43600 Bangi, Malaysia

*Author for correspondence (marjoniimamora@gmail.com)

MS received 15 June 2021; accepted 12 August 2021

Abstract. Anisotropic nanostructures, such as nanosheets, nanorods, etc., in many cases, generate superior physicochemical properties over a highly symmetric structure counterpart. Here, we present a straightforward method to grow vertically oriented ZnO nanosheet directly on fluorine-tin oxide substrate using a microwave-assisted quasi-hydrothermal method. We also found that the Ag nanoparticles (AgNPs) loading on the surface can effectively modify their optical properties, the potential for upgrading its performance in the existing applications. Due to the simplicity of the technique, AgNPs-loaded standing ZnO nanosheet should find potential application in solar cells, sensing and photocatalysis.

Keywords. Standing nanosheets; ZnO nanostructure; Ag nanoparticles; microwave-assisted hydrothermal.

1. Introduction

The morphology of the nanocrystals gives a strong influence on the overall properties of the materials [1–3]. This is the result of the modification of the confinement potential of the charge carrier when the shape of the nanocrystals is distorted under the quantum regime [4]. For example, in the case of Au or Ag nanoparticles (AgNPs), their surface plasmonic resonance changes from single localized surface resonance to two localized surface plasmon resonance characters, when their morphology transformed from spherical nanoparticles to nanorods or nanoplates morphology [5–8]. A similar case is also encountered in the ZnO nanocrystals [9,10]. For example, its excitonic photoluminescence properties redshifted from 369 to 371 nm when its morphology altered from spherical to nanorods, respectively [11]. Not only excitonic-related photoluminescence shift but also the nature of defect-related photoluminescence, i.e., blueshifted from 528 to 514 nm when the nanostructure shape changes from spherical to nanorods, respectively. In addition, owing to the alteration of the surface atom when the morphology of the nanostructure changes, their surface physicochemical properties are strongly transformed. This results in the enhancement of the surface reactivity in sensing [12], photocatalysis [13,14], surface biological activity [15,16] and solar cells [17] when the morphology of ZnO nanostructure is modified from highly symmetrical spherical morphology to anisotropic shapes, such as nanorods, nanoplates, etc. [18]. Considering the nature of physicochemistry transformation under morphology shift, the attempt to continuously prepare ZnO nanostructure with exotic anisotropic morphology should be demonstrated.

In this study, a simple and rapid method to grow a standing nanosheet of ZnO directly on the substrate surface is demonstrated via a microwave-assisted quasi-hydrothermal method [19]. In the typical process, the standing nanosheet has a length up to 1 μm and the thickness of the nanosheet is approximately 10 nm. The nanosheet growth direction on the surface is random, producing a pore-like surface, the result of the nanosheet network on the surface. We also found that the optical property of the standing ZnO nanosheet (SZN) significantly modified upon being decorated with AgNPs of size from 15 to 20 nm on their surface, which is hardly achieved in other systems such as nanorods or other morphologies. An optical energy gap red-shifting up to 0.04 eV was observed, signifying its potential for improved photoactivity properties in the application. The AgNPs loaded standing nanosheet of ZnO may find use in solar cells and non-linear optics applications.

2. Experimental

2.1 *AgNPs-loaded SZN preparation*

AgNPs-loaded SZN (Ag-SZN) on a fluorine-doped indium tin oxide (FTO) substrate were prepared by a two-step process, i.e., SZN growth and AgNPs loading onto the SZN structure. The SZN on FTO substrate (Sigma-Aldrich, the sheet resistance of ca. 10 Ω per square) was prepared by using our previously reported technique, namely microwave-assisted hydrolysis seed-mediated growth process [19]. Briefly, a cleaned FTO substrate that has been undergone a standard cleaning process in acetone and ethanol under an ultrasonication was sputtered with a thin layer of Al film (thickness approximately 30 nm) using an RF Magnetron Sputter machine. After following a further brief-cleaning process under ultrasonication in ethanol, ZnO nanoseeds of size approximately from 3 to 10 nm were deposited on the Al layer using alcohothermal seeding method [20], namely consecutive spin-coating of ethanolic solution of zinc nitrate hydrate, $ZnNO_3{\cdot}6H_2O$ (Alfa Aesar) and thermal annealing (using a split-tube furnace system (Thermcraft, USA)) at 200°C in air for 1 h. The SZN was then grown by simply immersing the FTO/Al-loaded ZnO nanoseed substrate into a growth solution that contains an equimolar (0.3 M) aqueous solution of $ZnNO_3{\cdot}6H_2O$ and 0.03 M hexamethylene tetramine. The growth reaction was carried out under microwave irradiation (power ca. ∼1100 W) inside a microwave oven (Panasonic) for 20 s. The sample was then taken out, washed in a copious amount of pure water, and dried using a flow of nitrogen gas. The as-prepared SZNs were then annealed for 1 h in the air at 350°C to remove any organic residue on the sample and to obtain a better ZnO crystallinity. From this procedure, a high-density SZN structure on the FTO substrate (confirmed by X-ray diffraction (XRD) and field emission scanning electron microscopy (FESEM) results) was obtained. In this study, the SZN with five different porous densities were prepared by simply varying the Zn precursor ($ZnNO_3{\cdot}6H_2O$) concentrations in the reaction, namely 0.01, 0.02, 0.03, 0.04 and 0.05 M. Other reagents and procedures used in this work were kept unchanged.

The Ag nanoparticle (AgNPs)-loaded SZN (Ag-SZN) were prepared by firstly immersing the SZN-coated FTO substrate into a 20 ml aqueous solution that contains 0.5 ml of 0.01 M $AgNO_3$ (Sigma-Aldrich, USA) and 0.5 ml of 0.01 M trisodium citrate (WAKO Chemical, Japan). The sample was left for 30 min undisturbed to facilitate Ag^+ ions adsorption onto the SZN surface. After that, 0.1 ml of ice-cooled $NaBH_4$ (0.1 M) was injected into the solution. The colour of the solution changed from colourless to yellow, indicating the formation of Ag both in the solution and on the surface of SZN. The reaction was then left undisturbed for another 1.5 h at room temperature, to facilitate the effective growth of AgNPs on the surface of SZN. The sample was then taken out, washed with a copious amount of pure water, and dried with a flow of nitrogen gas. Finally, the sample was annealed in air at 200°C for 1 h to remove any organic residue on the sample surface.

2.2 *Characterizations*

The morphologies of the unloaded and Ag-SZN were obtained using a field emission scanning electron microscopy (FESEM) Zeiss Supra 55VP FESEM apparatus. The phase and structural properties of the unloaded and Ag-SZN were characterized by X-ray diffraction (XRD) measurements using Bruker D8Advance with CuKα radiation (λ = 1.541 Å) and scan rate as low as 2° min^{-1}. UV-Vis diffuse reflectance spectroscopy (Winlab, Hitachi, Japan) was used to obtain the optical properties of the sample.

3. Results and discussion

3.1 *AgNP-loaded SZN*

Standing ZnO nanosheet with controlled porous density on the FTO substrate surface has been successfully prepared using the present method. Figure 1 shows the typical surface

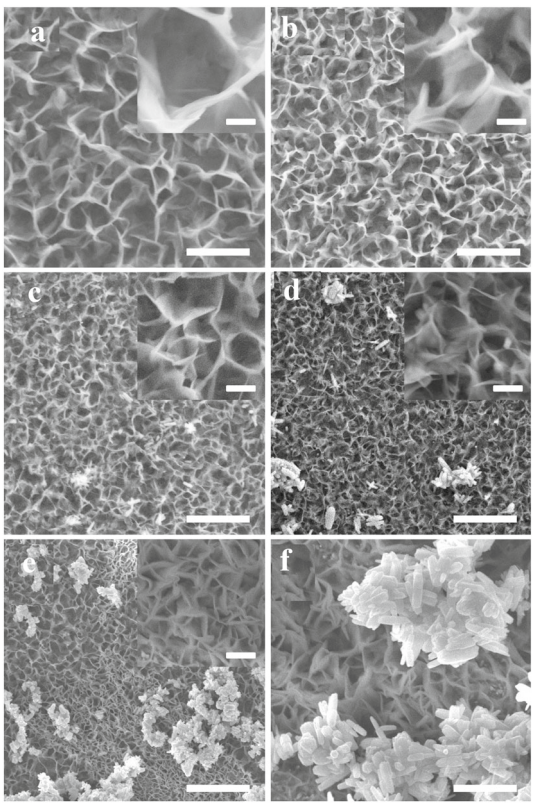

Figure 1. FESEM micrograph for SZNs morphology at various Zn^+ precursor molarities, namely (**a**) 0.01, (**b**) 0.02, (**c**) 0.03, (**d**) 0.04 and (**e**) 0.05 M. (**f**) A high magnification image for sample (**e**). Scale bars are 1 μm and 100 nm for insets and (**f**).

morphology of the SZN grown using five different Zn precursor concentrations, namely 0.01, 0.02, 0.03, 0.04 and 0.05 M. As shown in figure 1, the SZN is characterized by a continuously connected nanosheet structure that is vertically grown on the substrate surface, forming a porous surface structure. The thickness of the nanosheet is in the range of 10–15 nm and was found to have no significant dependency on the Zn precursors concentration used in the reaction. However, the pore size (the average edge-to-edge distance) decreases with the increase of ZnO precursor concentration in the reaction. For example, at low concentration (see figure 1a), the size of the pore is approximately 500 nm. The pore size effectively decreases when the precursor concentration was increased (figure 1a–e). At a relatively high concentration, i.e., 0.05 M (see figure 1e), the pore size is as low as ca. 50 nm. This produces SZN with high-pore density on the substrate surface, promising unique optical and electrical properties. A complete porosity data of nanosheet film grown from different ZnO precursor concentrations is summarized in table 1. The increase in the pore density upon the increasing of ZnO precursor concentration is simply related to the high-kinetic nature of the growth reaction at high precursor concentration, causing rapid growth and deposition of the ZnO nanostructure onto the surface [21,22]. Therefore, at this condition, the competitive nucleation characteristic of the reaction is high, resulting in the formation of smaller pore size, thus increases the density. Unfortunately, as can be seen from the figure, the use of high ZnO precursor concentration has caused unstability in the reaction that was indicated by an active formation of ZnO by-product in solution (ZnO nanorods), of which some of them are attached to the nanosheet surface. This could more or less distort the unique property of the porous nanosheet film. The results are shown in figure 1e and f (magnified images).

The formation of nanosheet structure has been understood as the effect of effective etching and passivation of (101) and (100) planes by the $Al(OH)_4^-$ complexes in the solution that is produced from the dissolution of the Al layer by hexamethylene tetramine [19]. This condition favours the growth of two-dimensional morphology instead of other morphologies, such as spherical or irregular shape nanostructures.

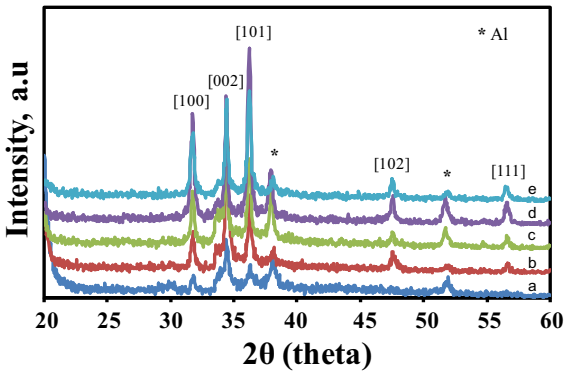

Figure 2. XRD spectra for SZNs morphology at various Zn^+ precursor molarities of (**a**) 0.01, (**b**) 0.02, (**c**) 0.03, (**d**) 0.04 and (**e**) 0.05 M.

Figure 2 shows the phase analysis result of the SZN that were prepared using five different Zn^+ precursor solutions, namely 0.01, 0.02, 0.03, 0.04 and 0.05 M. As can be seen from the figure, the entire sample shows a similar XRD pattern with the presence of five major peaks in the spectrum, namely at 2θ of 31.6, 34.3, 36.2, 47.5 and 56.6°. This XRD pattern agrees well with the standard XRD data (file no. 36-1451) for the pure ZnO phase with peaks at 2θ of 31.6, 34.3, 36.2, 47.5 and 56.6° corresponding to the XRD from the (100), (002), (101) (102), and (111) Bragg planes, respectively. It can be noted here that the SZN produce from the lower precursor concentration seems to be characterized by the (002) plane (*c*-axis plane) because of a high-diffraction intensity originated from this plane (see curve *a*). However, the XRD profile was effectively modified when the SZN was prepared using a higher ZnO precursor concentration (see curves *b* to *e*). At these concentrations, the SZNs were characterized by (101) plane with ratio diffraction intensity between (101) and (002) planes as high as 1.5, which is only 0.5 for sample *a*. It is also observed that the diffraction from the (100) plane is also high and comparable to the (002) plane with an intensity ratio between (100) and (002) in the range of 0.6 to 0.8, which is only 0.4 for the sample *a*. We assumed that the SZN wall should be characterized by the planes of (101) and (100). As the (101) and (100) planes for ZnO is a highly energetic surface, thus we expect peculiar optical and

Table 1. Average pore diameter for SZNs prepared at five different concentrations.

Zn precursor concentrations (M)	Average pore diameter (μm)	Optical band edge (eV)
0.01	1.683	3.310
0.02	1.350	3.305
0.03	0.941	3.290
0.04	0.729	3.290
0.05	0.654	3.290

electrical properties to be produced from this structure. In addition, from the spectra, the Al crystal peaks were also present, namely at 38.0° and 56.5°. This could be from the Al layer that is not completely consumed during the SZN formation. However, their intensity is relatively low and its effect on the optical and electrical properties of SZN is expected to be minimum.

We then grew AgNPs onto the surface of SZN by our previously reported technique that involves a simple immersion of the SZN sample into the solution of Ag colloidal reaction formation. After finishing the AgNP growth procedure for 1.5 h and followed by brief rinsing using pure water, we carried out a FESEM analysis to confirm the AgNPs formation on the SZN surface. The result is shown in figure 3. As shown in figure 3, the AgNPs have been effectively attached to the surface of the SZN. They are indicated as bright dotted particles as shown in the high-resolution FESEM image in the inset of the corresponding FESEM image (see figure 3a–e). Their size range from 15 to 20 nm. The elemental analysis using electron energy dispersion spectroscopy (EDS) might further verify the AgNPs existence on the surface of SZN. Nevertheless, due to the limited access to the technique, we cannot provide them at this stage. However, the presence of such bright nanoparticles on the surface of SZN after a treatment in the AgNPs colloidal reaction is a clear indication that the AgNPs successfully decorate the SZN. Notwithstanding, the XRD and optical absorption analyses (will be discussed in the following) have confirmed that the AgNPs are existing in SZN thin films.

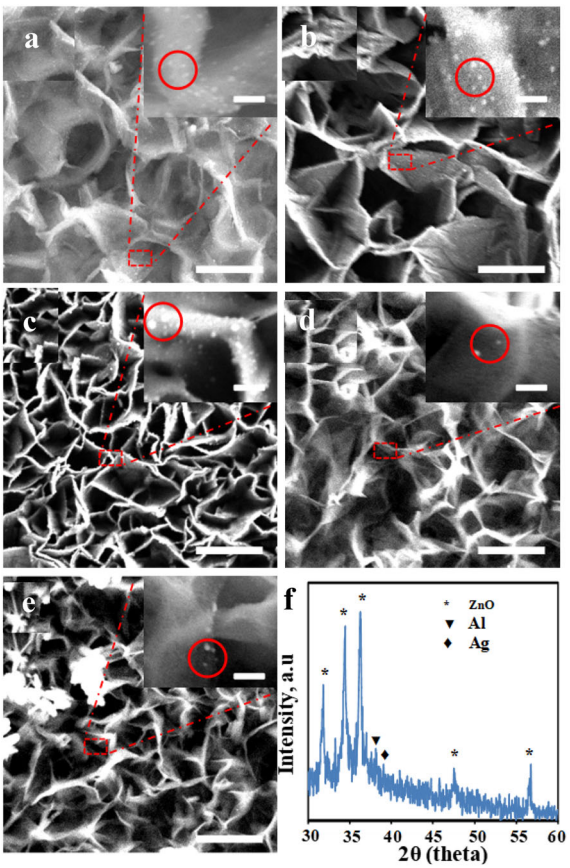

Figure 3. (**a**–**e**) FESEM image of vertical ZnO nanosheet from different precursor concentrations, as in figure 1, decorated with AgNPs. Panel (**f**) is the XRD pattern of the sample. Scale bars are 1 μm and 100 nm in the inset.

We then performed an XRD analysis of the sample to further verify the existence of the AgNPs in the sample. A sample with medium Zn precursor concentration, i.e., 0.03 M, was used in the analysis. As has been expected, the Ag crystalline phase is observed in the XRD spectrum along with the ZnO and Al (see figure 3f). The SZN decorated with AgNPs should produce special properties so that unusually high performance in the application would be obtained. As shown in figure, the peak intensity of the AgNPs is indeed weak if compared even with the Al. Because the XRD peak intensity is related to the crystallite size ratio of the component in the sample where SZN, particularly, majorly composes the sample, the diffraction peaks are dominated by the SZN leaving other crystallite components weakly observed in the XRD pattern. The Al peak intensity is higher than the AgNPs, which could be due to the same reason where Al layer crystallite size is bigger than AgNPs. It is because Al layer is not completely consumed during the catalytic projection of SZN. The Al layer was deposited on the entire surface of the substrate with a thickness of approximately 30 nm. An incomplete consumption of Al layer during the growth of SZN could leave the Al layer with crystallite size higher than AgNPs (size approximately 15 nm). Thus, the Al layer XRD peak is higher than AgNPs.

We carried out a UV-Vis absorption spectroscopy technique to further verify the presence of AgNPs on the surface of SZN and to evaluate the optical properties of the SZN under the influence of AgNPs attachment. Figure 4a shows their corresponding optical absorbance. It is seen that excitonic absorption of ZnO (at the wavelength of ca. 360 nm) [23] along with localized surface plasmon resonance absorption of Ag (ca. 419 nm) [24] are observed in the spectrum. This certainly is a further confirmation of the AgNP's existence on the surface of SZN. As can be seen from figure 4b and table 1, it can be estimated that there is a modification in the optical bandgap of the SZN when its dimension is altered due to the dimensional effect at this nanostructure regime or decorated with the AgNP. We then extrapolate the Tauc plot from the absorbance spectrum of the sample to see the impact of dimension modification and the AgNP attachment on the optical properties of the SZN (see figure 4b). For example, the thinnest SZN (curve 1 in figure 4b) decorated with the AgNPs has an optical band edge as high as 3.31 eV. It gradually decreases with the increase of thickness and has an optical energy gap as low as 3.29 eV in the thickest ZnO nanosheet (curve 5 in figure 4b). Because the AgNPs dimension and density on the SZN surface are more or less similar on each SZN

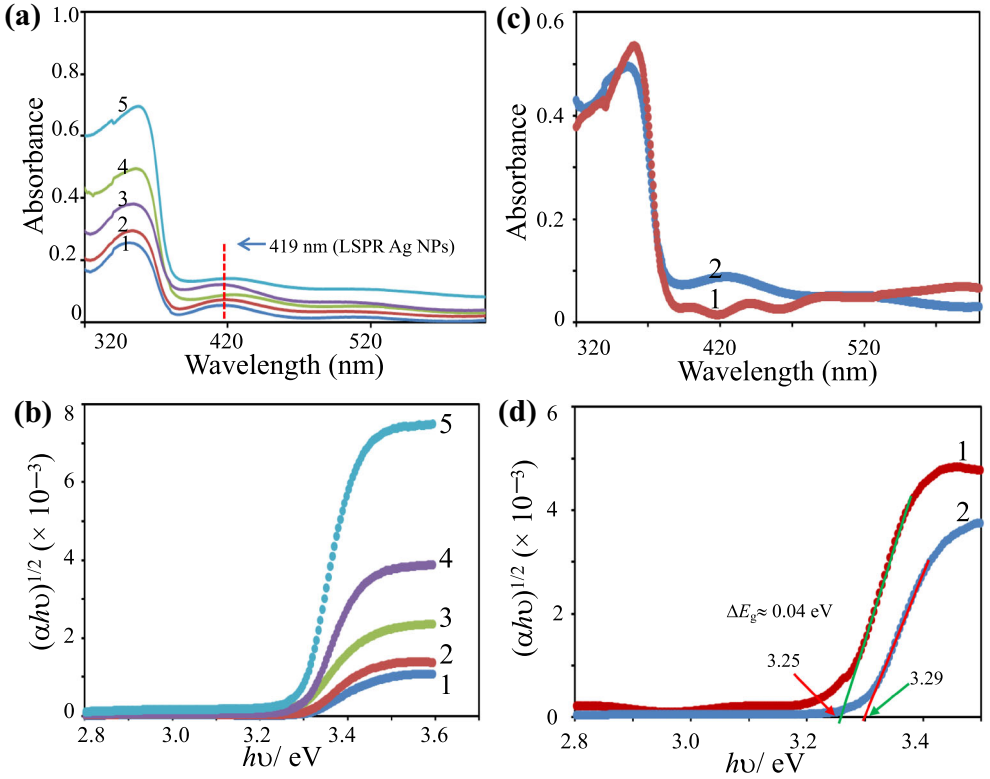

Figure 4. (**a**) Optical absorbance of the vertical ZnO nanosheet decorated with AgNPs with different ZnO precursor concentrations, i.e., 0.01 (1), 0.02 (2), 0.03 (3), 0.04 (4) and 0.05 M (5). (**b**) Corresponding Tauc plot of the samples. (**c**) Comparison of optical absorption properties of pristine ZnO nanosheet (curve 1) and AgNPs decorated ZnO nanosheet (curve 2), and (**d**) their corresponding Tauc plot showing modification on the optical bandgap.

sample, as expected, we can remark that the energy gap decrease should be due to the increase in SZN dimension and thickness [25]. To understand the extent effect of AgNP impact on the optical properties of the SZN, we compared the optical properties of pristine SZN with the ones decorated with AgNPs that were prepared using similar ZnO precursor concentration (0.04 M). The result is shown in figure 4c and d. We noticed that the band edge of the ZnO is blue-shifted up to 0.04 eV with the attachment of AgNPs (figure 4d). The pristine SZN optical band edge is approximately 3.25 eV. This result is quite surprising as surface attachment of the AgNPs in fact can induce the bulk optical properties of the SZN, which could be via many ways such as carrier equilibration effect, Fermi level alignment between the Ag and ZnO, etc. Normally, such transformation in the bulk optical properties of material should be produced by a strong perturbation from the external agent, in this case, the AgNPs [26]. However, considering the low thickness of the SZN, i.e., approximately 15 nm, bulk electronic modification in the SZN by the AgNPs attachment would be possible. This certainly is followed by modification of the overall physicochemistry properties of the SZN. Enhanced performance in the existing application is expected from the Ag-decorated SZN.

We again remark that the AgNPs have effectively modified the optical properties of SZN, which was achieved via a two-step process. We predict that, although the present result uses FTO as the substrate, the method should also be extended to grow SZN on other substrates, such as glass. While the two-step method could be a tricky and lengthy process, notwithstanding, it offers a sophisticated way to attain a preserved morphology of the SZN and the AgNPs. A simple, one-pot reaction process has been used to grow and modify the electrical and optical properties of the ZnO nanostructure as in the formation of Ag-ZnO nanorod [27]. Nevertheless, although it might produce effective modification on the optical properties of ZnO nanostructure, it may induce a deformation on the two-dimensional crystal growth in the ZnO. Therefore, a special effort could be conducted to realize a one-pot process for the preparation of AgNPs-decorated SZN.

Nevertheless, the Al system is still detected in the sample with significant content as shown in the XRD analysis result. This is the result of the Al layer that is not fully consumed during the catalytic growth of SZN. It may certainly generate a strong effect on the optical and electrical properties of the SZN. At this stage, the approach to remove or decrease the Al content in the SZN is not yet obtained.

We assumed that the use of appropriate thickness of Al layer or the use of an additional catalyst to accelerate the Al consumption might remove or reduce the Al presence in the SZN. This effort is being pursued and the result will be reported separately.

4. Conclusions

The method to prepare SZN on the substrate surface has been presented via the microwave-assisted hydrothermal method. The SZN has a length of up to 1 μm and thickness can be as low as 10 nm. We also discovered that the AgNPs of size up to 20 nm can induce change in the optical absorption properties of the SZN. In the typical process, the optical energy band edge of the SZN blue shifts as high as 0.04 eV upon being decorated with the AgNPs. This is unusual and is assumed due to the thin structure of the nanosheet so that the AgNPs attachment on the surface can strongly distort both the surface and the bulk lattice of the SZN. This system should find extensive application in sensors, photocatalysis and solar cells.

Acknowledgements

We thank the Ministry of Higher Education of Malaysia for supporting this project under FRGS/1/2019/STG02/UKM/02/3 grant.

References

[1] Polarz S 2011 *Adv. Funct. Mater.* **21** 3214
[2] Burda C, Chen X, Narayanan R and El-Sayed M A 2005 *Chem. Rev.* **105** 1025
[3] Mclaren A, Valdes-Solis T, Li G and Tsang S C 2009 *J. Am. Chem. Soc.* **131** 12540
[4] Alivisatos A P 1996 *Science* **271** 933
[5] Ali Umar A and Oyama M 2005 *Cryst. Growth Des.* **5** 599
[6] Ali Umar A and Oyama M 2006 *Cryst. Growth Des.* **6** 818
[7] Ali Umar A and Oyama M 2008 *Cryst. Growth Des.* **9** 1146
[8] Ali Umar A, Oyama M, Mat Salleh M and Yeop Majlis B 2010 *Cryst. Growth Des.* **10** 3694
[9] Viswanatha R, Sapra S, Satpati B, Satyam P, Dev B and Sarma D 2004 *J. Mater. Chem.* **14** 661
[10] Schoenhalz A L, Arantes J T, Fazzio A and Dalpian G M 2010 *J. Phys. Chem. C* **114** 18293
[11] Zhao J-H, Liu C-J and Lv Z-H 2016 *Optik* **127** 1421
[12] Quy C T, Hung C M, Van Duy N, Hoa N D, Jiao M and Nguyen H 2017 *J. Electron. Mater.* **46** 3406
[13] Mintcheva N, Aljulaih A A, Wunderlich W, Kulinich S A and Iwamori S 2018 *Materials* **11** 1127
[14] Tan S T, Ali Umar A, Balouch A, Yahaya M, Yap C C, Salleh M M *et al* 2014 *ACS Comb. Sci.* **16** 314
[15] Orou S F C, Hang K J, Thien M T, Ying Y L, Diem N D N, Goh B H *et al* 2018 *J. Ind. Eng. Chem.* **62** 333
[16] Al-Hinai M H, Sathe P, Al-Abri M Z, Dobretsov S, Al-Hinai A T and Dutta J 2017 *ACS Omega* **2** 3157
[17] Rahman M Y A, Umar A, Taslim R and Salleh M M 2013 *Electrochim. Acta* **88** 639
[18] Tan S T, Umar A A and Salleh M M 2016 *J. Phys. Chem. Solids* **93** 73
[19] Ridha N J, Umar A A, Alosfur F, Jumali M H H and Salleh M M 2013 *J. Nanosci. Nanotechnol.* **13** 2667
[20] Tan S T, Umar A A, Balouch A, Yahaya M, Yap C C, Salleh M M, Oyama M *et al* 2014 *Ultrason. Sonochem.* **21** 754
[21] Viswanatha R, Amenitsch H and Sarma D 2007 *J. Am. Chem. Soc.* **129** 4470
[22] Viswanatha R, Santra P K, Dasgupta C and Sarma D 2007 *Phys. Rev. Lett.* **98** 255501
[23] Laskowski R and Christensen N E 2006 *Phys. Rev. B* **73** 045201
[24] Nafisah S, Saad S, Umar A A, Plucinski K, Lis M, Maciaga A *et al* 2015 *Opt. Appl.* **45** 263
[25] Miao L, Tanemura S, Tanemura M, Lau S P and Tay B 2007 *J. Mater. Sci. Mater. Electron.* **18** 343
[26] Hewlett R M and McLachlan M A 2016 *Adv. Mater.* **28** 3893
[27] Sarkar S and Basak D 2013 *CrystEngComm.* **15** 7606